Journal of Molecular Catalysis A: Chemical 353–354 (2012) 74–79

Contents lists available at SciVerse ScienceDirect

Journal of Molecular Catalysis A: Chemical

journal homepage: www.elsevier.com/locate/molcata

Photocatalytic reduction of Cr(VI) on the new hetero-system $CuCr_2O_4$/ZnO

H. Lahmar[a], M. Kebir[b], N. Nasrallah[b], M. Trari[a,*]

[a] Laboratory of Storage and Valorization of Renewable Energies, Faculty of Chemistry USTHB, BP 32, Algiers, Algeria
[b] Laboratory of Engineering Reaction, Faculty of Mechanic and Engineering Processes USTHB, BP 32, Algiers, Algeria

ARTICLE INFO

Article history:
Received 28 May 2011
Received in revised form 29 October 2011
Accepted 31 October 2011
Available online 12 November 2011

Keywords:
Chromate
Photoreduction
Spinel $CuCr_2O_4$
ZnO
Hydrogen
Solar

ABSTRACT

Self photodriven chromate reduction and oxalic acid oxidation are concomitantly achieved over the new hetero-system $CuCr_2O_4$/ZnO. The absorption of light promotes electrons in the sensitizer conduction band ($CuCr_2O_4$-CB) with a potential (−0.95 V_{SCE}), too negative to be involved in an electron exchange with $HCrO_4^-$ species. The improved activity is due to the electron injection from activated $CuCr_2O_4$ into ZnO-CB (−0.58 V_{SCE}). The nitrate route is suitable to prepare active ZnO on which the chromate reduction occurs. A reduction of more than 60% of $HCrO_4^-$ is achieved in air equilibrated solution under optimal conditions (pH∼3.5, 1 mg catalyst mL^{-1}, 25 °C). The experimental data are fitted adequately with the modified Langmuir–Hinshelwood model. The reduction follows a pseudo first order kinetic with a half life of 53 min for a concentration of 10^{-4} M. The oxidation of Cr^{3+} by photo holes and the competitive water reduction are though to be the main reasons of the regression in the photoactivity. The hetero-system favours hydrogen formation, with a rate evolution of 15 μmol h^{-1} mg^{-1}.

1. Introduction

Thanks to the depletion of fossil energies reserves, a great interest in the renewable energetic sources exists really [1,2]. Over the last decades, increasing concern with alternate solar power has been focused on ecological objectives and mainly on water pollution issues [3]. So, the photoelectrochemistry has extended its field to the elaboration of optically active materials concerning the environmental protection [4]. It is now well established that hexavalent chromium is a carcinogenic product which is accumulated in living organisms. Large amounts are discharged in water by many industries like leather tanning, manufacturing, processes, electroplating and textiles. Cr(VI) exists at concentrations ranging from 50 ppm to 200 ppm and as the water quality becomes more difficult to get exacting, there has been renewed interest in the techniques for its removal. Cr(VI) is not biodegradable and must be eliminated at the source [5]; its concentration must be less than 5 ppm as required by environmental standards in water pollution. The conventional processes including ion exchange, activated carbon, reverse osmosis and membranes are either expensive or difficult to use [6]. Each technique has its own shortcomings and often does not comply with the threshold set up by the World Health Organization. In addition, some of them are inefficient at low concentrations and can be used as post treatment in photocatalysis.

The photo electrochemical (PEC) conversion works under mild operating conditions and is particularly attractive when the solar constant averages 1.3 kW m^{-2} (Algeria). It has proven its usefulness in the reduction of Cr(VI) into trivalent state which can be safely recovered by precipitation and/or chelated on various substrates [7]. In this regard, many semiconductor (SC) oxides have been used to convert a variety of inorganic pollutants into less harmful forms [8]. Unfortunately, the energy required to excite electrons from the valence band (VB) to the conduction band (CB) is greater than 3 eV and the corresponding wavelengths lie in the UV region of the solar spectrum which accounts only 4%. To these losses must be added those due to low absorption which are more pronounced for indirect transitions. On the other hand, the major handicap with non oxide SC is their susceptibility to photocorrosion. The optical gap (E_g) and the flat band potential (V_{fb}) are two crucial parameters which govern the quantum efficiency of PEC devices. Up to now, little attention has been paid to the spinels family CuM_2O_4 despite their chemical stability and optical gap close to the ideal value required in terrestrial applications [9], M being a *3d* metal. The reduction of the gap occurs at the expense of change of VB due to the more energetic t_{2g} orbital which decreases the E_g value to approximately 1.6 eV [10]. More recently, CuM_2O_4 are found to be active sensitizers in the water reduction [11] where the overvoltage may be overcome owing to the cationic character of the electronic bands and this is not the case of most oxides. The potential of CB can be properly matched with respect to redox levels in order to allow a fast electron exchange otherwise the kinetic

* Corresponding author at: Laboratory of Storage and Valorization of Renewable Energies, Faculty of Chemistry USTHB, BP 32, Algiers, Algeria.
Tel.: +213 21 24 79 50; fax: +213 21 24 80 08.
E-mail address: solarchemistry@gmail.com (M. Trari).

1381-1169/$ – see front matter © 2011 Elsevier B.V. All rights reserved.
doi:10.1016/j.molcata.2011.10.026

of electron transfer becomes very slow and the photocorrosion takes place. The difference ($E_{red} - V_{fb}$) exceeds 1 V and inhibits the electrons exchange leading to weak PEC performance. However, the potential of CuM_2O_4-CB is pH insensitive whereas that of ZnO usually varies by – 0.06 V pH^{-1} and we have used this property to get an optimal band bending at the interface. Enhanced photoactivity is attributed to the electron transfer from the sensitizer $CuCr_2O_4$-CB, activated by visible light, to ZnO-CB resulting in the chromate reduction. The photo oxidation of organic compounds is a clean strategy which contributes significantly to the metals recovery because of the longer lifetime of the charge carriers. The process leads to a total mineralization without leaving any hazardous residues [11]. Bearing in mind the recent success of the spinels with nano size dimensions and large reaction cross sections [12], we may hope to find a better photoactivity over $CuCr_2O_4$ prepared by co precipitation.

Besides, the current energy sources come mainly from fossil fuels which are being depleted rapidly by the increasing industrial activities. Another application of the spinels is their use in the light energy storage through the environmental friendly hydrogen [11]. The exploitation of the solar energy reduces greenhouse gas emission, which is responsible for the climate change. Water competes with the $HCrO_4^-$ ions for the photo electrons and the reduction decelerates over time favouring the hydrogen formation.

2. Experimental

2.1. Catalysts preparation

Stochiometric amounts of $Cu(NO_3)_2$ (Merck, 99%) and $Cr(NO_3)$, $4H_2O$ (Fluka >99%) are dissolved in water and the nitrate excess is decomposed at 300 °C on a magnetic-stirring hot plate. The amorphous powder is homogenized in an agate mortar and fired at 950 °C. ZnO is prepared by dissolving $Zn(NO_3)_2{,}6H_2O$ (Merck, 99.5%) in water, the solution is deshydrated and denitrified at 200 °C. The powder is heat-treated at 500 °C and the oxide shows a pale yellowish color. The end products are identified by X-ray diffraction (XRD) using Cu Kα radiation (λ = 0.15418 nm) in the 2θ range (5–80°). The diffuse reflectance spectrum is measured with a double beam spectrophotometer (Cary 500) equipped with an integrating sphere:

$$\text{Abs} = \log\left[\frac{\text{Reflectance of MgO}}{\text{Reflectance of } CuCr_2O_4}\right] \quad (1)$$

The powder is cold pressed under 3 kbar and sintered at 1000 °C, the pellets have more than 90% of the theoretical density. The ohmic back contact is made by using silver paint and the exposed surface is 0.5 cm^2. PEC characterization is performed in a standard electrochemical cell, Pt electrode (Tacussel) serves as an auxiliary electrode and the potentials are given with respect to a saturated calomel electrode (SCE) and monitored by a PGZ301 potentiostat (Analytical Radiometer). The double walled photoreactor (100 mL capacity) containing aerated powder suspension is the same as that used in our previous study [11]. The stock solution is prepared by dissolving $K_2Cr_2O_7$ (Merck, 99.5%) in bidistilled water at the concentration of 30 ppm. The catalyst dosage is fixed at 1 g {((1 − x) $CuCr_2O_4$/x ZnO)} L^{-1} and the pH is adjusted by addition of H_2SO_4 and controlled with a digital pH meter (Schott 825). The temperature is regulated by a thermostated bath (Julabo). Above 50 °C, evaporation occurs more considerably than the chromate removal. The experiments are conducted under illumination of a tungsten lamp (200 W) emitting in the wavelength range of 400–950 nm, with a maximum at 650 nm; the radiant flux is measured with a commercial radiometer (Testo 545) and may be varied by moving the lamp closer to or farther from the reactor. The light is turned on after a transition period to ensure $HCrO_4^-$ adsorption and the powder is suspended under constant magnetic stirring. The aliquots are taken at regular times for the kinetic study. The solution is centrifuged to separate the catalyst particles from the solution; the filtrate is systematically acidified by H_2SO_4 and analyzed by measuring the absorbance at 350 nm in 1 cm path length quartz cell with UV–visible spectrophotometer (Shimadzu UV 1800). The concentration is checked by potentiometric titration with the Mohr salt. No change in absorbance is observed in the dark. The details of the experimental set up used for the hydrogen evolution have been given in a previous work [11].

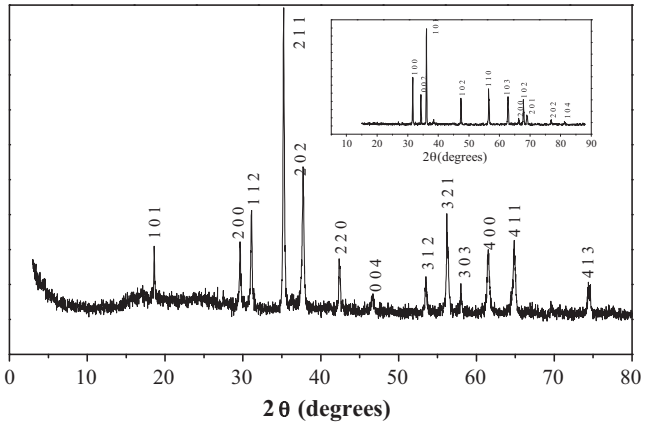

Fig. 1. XRD patterns of $CuCr_2O_4$ and ZnO (Inset) synthesized by nitrate route.

3. Results and discussion

The XRD patterns (Fig. 1) show that the synthesized samples are single phases. The spinel $CuCr_2O_4$ crystallizes in a tetragonal symmetry with the lattice constants: $a = 6.0247$ and $c = 7.4619$ nm in agreement with the JCPDS card No. 34-0424. ZnO exhibits a good crystallinity (Inset) and all the peaks index on the basis of a hexagonal structure (JCPDS card No. 36-1451). The diffuse reflectance data of $CuCr_2O_4$ (Fig. 2a) are converted into absorptivity, using the Kubelka–Munk function:

$$F(R_\infty) = \frac{(1 - R_\infty)^2}{2R_\infty} \quad (2)$$

where $R_\infty = (I/I_o)_{dif}$ is the diffuse reflectivity from a thick layer (2 mm). The plot of $\log(I_o/I_{dif})$ against wavelength gives an acceptable representation of the spectrum, the plot $(\alpha h\nu)^2$ against the incident energy indicates an optical transition directly allowed at 1.40 eV(Inset). Both VB and CB derive from *3d* orbital, thus the light absorption is considered as *d–d* transition.

Activated conductivity is found in $CuCr_2O_4$ that we attribute to a small polaron hopping. The thermal evolution of the conductivity $\sigma(T)$ obeys to an Arrhenius type law (Fig. 2b) with activation energy E_a of 0.11 eV. We have characterized the spinel photoelectrochemically in order to get additional information on the energy band diagram. The potential V_{fb} is determined from the interfacial capacitance using the Mott–Schottky relation:

$$C^{-2} = \pm\frac{2}{e\varepsilon\varepsilon_o S N_A}\left\{V - V_{fb} - \frac{kT}{e}\right\} \quad (3)$$

where S is the surface area of the electrode and the other symbols have their usual significations. The curve (C^{-2}–V) exhibits a good linearity (Fig. 3a); the potential V_{fb} (−0.34 V) is obtained by extrapolating the plot to $C^{-2} = 0$. The holes density N_A (4.48×10^{18} cm^{-3}) is determined from the slope that its negative value is characteristic of *p* type conductivity. The permittivity ε (∼10) is determined from the dielectric measurement on sintered pellet. $CuCr_2O_4$ is doped moderately inducing a wide space charge region with the photoeffect

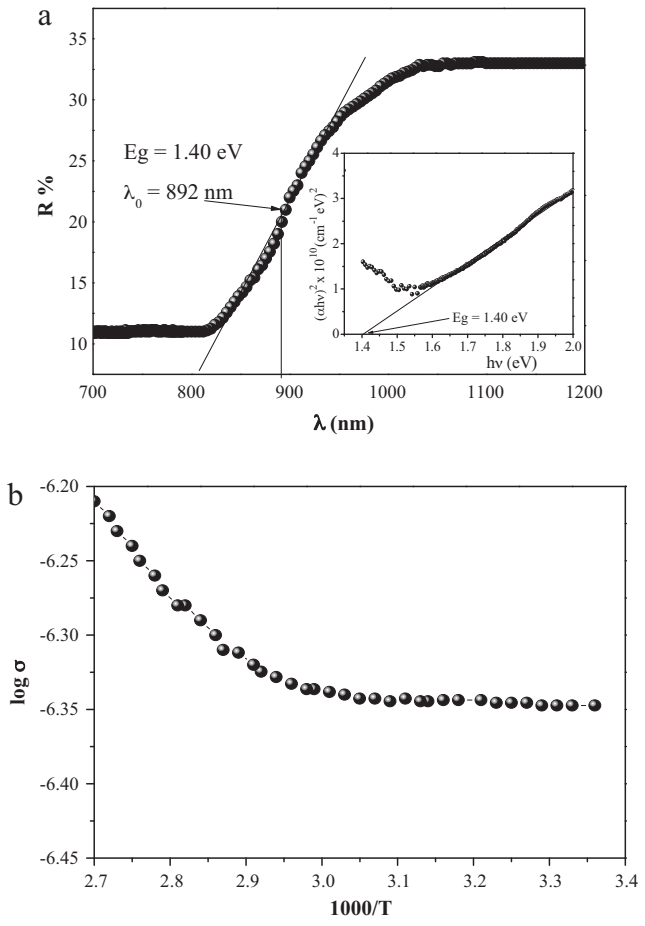

Fig. 2. (a) The diffuse reflectance spectrum of $CuCr_2O_4$. Inset: direct band gap transition. (b) The thermal variation of the electrical conductivity of $CuCr_2O_4$.

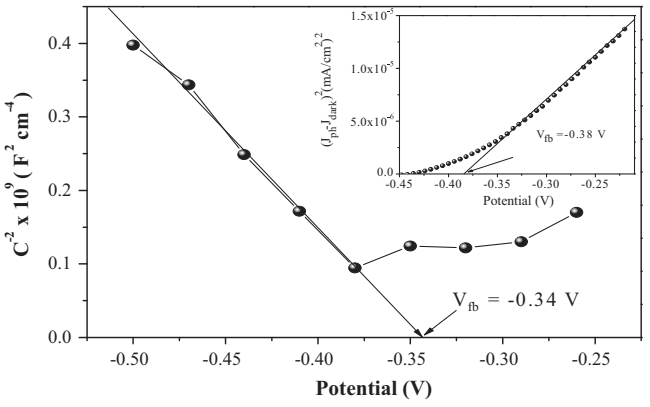

Fig. 3. The Mott–Schottky characteristic of $CuCr_2O_4$ plotted at a frequency of 10 kHz. Inset: the flat band potential of ZnO at pH 3.5.

occurrence. The depletion width ($W \sim 11$ nm)[1] extends over many crystallographic units and this is advantageous in photocatalysis. However, $CuCr_2O_4$ suffers from the low mobility originated from narrow CB which makes small the diffusion length of the minority carriers (electrons). As a result, the PEC process becomes kinetically governed by the electrons flow which is rate determining. Indeed, the photo current J_{ph} is unaffected by vigorous agitation of the solution lending a further support of the above point. So, the oxide has been prepared by chemical route. This has been done in order to shorten the traveled electronic path, giving a high probability to the electrons to reach the interface. The potential (V_{fb}) outlines the energetic position of VB with respect to vacuum:

$$eV_{fb} + E_a + 4.74 = 5.19 \pm 0.05\,\text{eV} \quad (4)$$

Such value is typical of oxides in which VB derives from cationic character instead of O^{-2}: *2p* orbital as it is the case of most oxides. Therefore, the CB potential (3.79 eV/−0.95 V) is located below the $HCrO_4^-/Cr^{3+}$ level which should lead to a spontaneous reduction. ZnO is stable down to pH 3 and the potential V_{fb} (−0.38 V), is roughly evaluated from the current potential curves according to the Gartner model (Fig. 3 inset). The physical and PEC characterizations of $CuCr_2O_4$ and ZnO (Table 1) allow us to draw the energy band diagram of the hetero-system (Fig. 4) which predicts from a thermodynamical point of view whether the $HCrO_4^-$ reduction and/or hydrogen evolution occurs or not.

3.1. Photocatalysis

Less attention has been paid for exploiting the PEC properties of spinels for other goals than the conversion of light into chemical fuels. Special interest has been paid lately to its utilization in the environmental protection which requires an elaboration of powder with a pollutant removal capability [13]. However, the question of longevity still remains open and a chemical inertness is required for long term applications. To assess the chemical stability, test up to 1 week of continuous immersion of $CuCr_2O_4$ powder is carried out in the working solution (pH ∼ 3.5), the amount of the dissolved copper would be too small for a reliable determination[2].

The primary step of the photocatalytic process consists of generating electron–hole (e^-/h^+) pairs that are available in the redox process. In acid solution, the free potential U_f of $CuCr_2O_4$ (−0.45 V) belongs to the immunity domain of $CuCr_2O_4$ in the potential-pH diagram and the specie $HCrO_4^-$ is predominant owing to the acidity constant ($pKa_1 = 6.49$) [14]:

$$HCrO_4^- + H_2O \leftrightarrow CrO_4^{2-} + H_3O^+ \quad (5)$$

The potential of Cr(VI) usually changes with pH: −0.14 V decade^{-1} and the rate to what extent it can be reduced is governed by the pH. The potential difference between the $HCrO_4^-/Cr^{3+}$ level and $CuCr_2O_4$-CB measures the band bending i.e. the driving force for the Cr(VI) reduction. However, the large value (∼1 V) makes the photoactivity weak and the process needs mediation of a wide band gap SC. As mentioned above, the main merit of the spinel is in the electronic bands invariance with pH and that it is used for this property. This would allow an adjustment of $CuCr_2O_4$-CB with respect to ZnO-CB, the latter varies by 0.059 V decade^{-1}. Besides, the photocatalytic performance of ZnO is hampered by the large gap (∼3.2 eV) which has showed no activity over 4 h illumination period. The photoactivity is directly related to the active surface of ZnO which shows a dark adsorption for $HCrO_4^-$. So, a transition time is needed before illumination. The potential of zero charge (pzc) of ZnO, the pH at which the net adsorbed surface is zero, is found to be 7.23 and the experiments are carried out in acidic medium where $HCrO_4^-$ species are attracted by the ZnO surface charged positively. The starting concentration is set at 30 ppm and the $HCrO_4^-$ solution is equilibrated with the catalyst during 2 h to establish the adsorption conditions. The difference between the nominal concentration

[1] The width is calculated from the relation: $W = \sqrt{\frac{2\varepsilon\varepsilon_0(V_{fb}-V)}{eN_D}}$ for a band bending of 0.5 V.

[2] Copper is titrated by iodometry with a standard $Na_2S_2O_3$ solution.

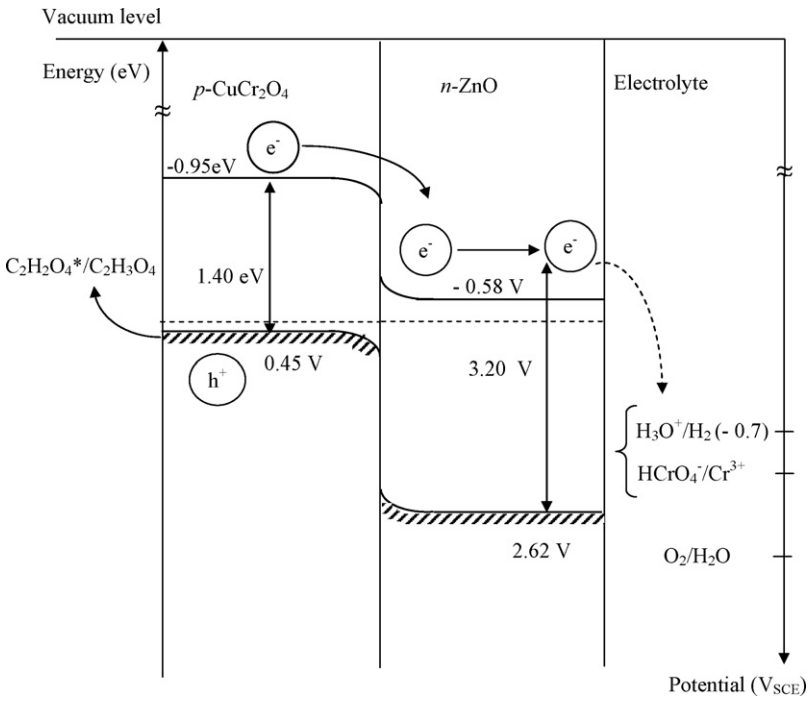

Fig. 4. Energy band diagram of the hetero-system $CuCr_2O_4/ZnO/Cr_2O_7^{-2}$ electrolyte.

and that of measured after equilibrium is taken as the quantity of adsorbed chromate onto the powder (~7%).

The hetero-systems allow the extension of the spectral photoresponse of wide band SCs toward the visible region where the sensitizer $CuCr_2O_4$ works as an electron pump. Thereafter, the straightforward explanation of the enhanced activity is that the electrons migrate to $HCrO_4^-$ via ZnO interfacial mechanism reaction. The chromate reduction on the *p*-$CuCr_2O_4$/*n*-ZnO junction is thermodynamically feasible but requires a large over-potential and light can be used in this purpose:

$$HCrO_4^- + 3/2C_2H_2O_4 + 4H^+ \rightarrow Cr^{3+} + 3CO_2 + 4H_2O \quad (6)$$

with a free enthalpy of −529 kcal mol^{-1} [15] and a spatial separation of two half electrochemical reactions.

The amount of reduced chromate depends on the light flux (Fig. 5). A linear behavior is observed at small intensities, the plot deviates from linearity above a critical value (20 mW cm^{-2}) and a clear tendency to saturation is observed. The well defined plateau region at high intensities indicates that the number of incident photons exceeds that of the catalytic sites and the reduction process becomes limited by the electrons flow within the diffusion length of $CuCr_2O_4$. The low diffusion rate is due to the narrowness of CB deriving from *3d* parentage which does not exceed 2 eV. So, it is interesting to work under direct solar irradiation with no concentrator where the diffuse nature of the sun allows low capital investments.

The photocatalytic tests are carried out with various mass concentrations C_m ($CuCr_2O_4$/ZnO) and the results, reported in Fig. 6, have given an optimal ratio of 1. For small C_m values, less active sites for the reduction process are available and the activity increases

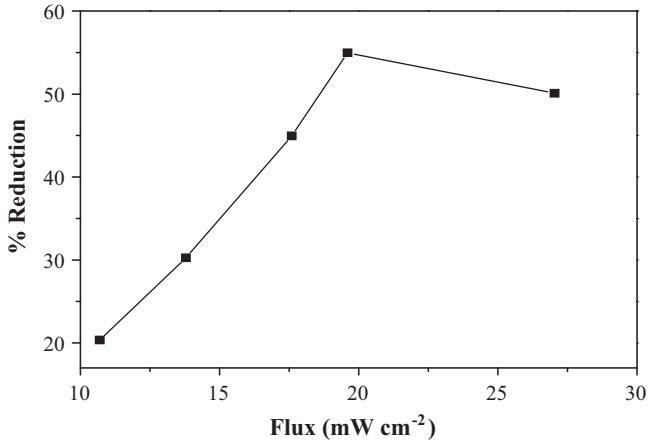

Fig. 5. The effect of intensity flux on the Cr(VI) reduction over the heterosystem $CuCr_2O_4$/ZnO.

nearly linearly with C_m. It decreases when further catalyst is added. The high turbidity of solution and the light penetration depth account for the regression of the activity. One way to prevent the accumulation of photocarriers i.e. to increase their lifetimes and to prevent the corrosion is to use hole scavenger and oxalic acid is particularly favourable. It reduces the recombination of (e^-/h^+) pairs, thus resulting in more efficient performance. Fig. 7 compares the UV–vis spectra of chromate under illumination. The decay in absorbance at 350 nm is due to a decrease of $HCrO_4^-$ light induced oxidation since no change in absorbance has been observed in the

Table 1
The main physical properties of $CuCr_2O_4$ and ZnO.

	Parameters (nm)	Crystallite size (nm)	SS (m^2 g^{-1})	σ (Ω cm)$^{-1}$	E_g (eV)	E_a (eV)	V_{fb} (V_{SCE})	E_{VB} (V_{SCE})	E_{CB} (V_{SCE})
$CuCr_2O_4$	Quadratic a = 6.024 c = 7.461	50	23	4.47×10^{-7}	1.40	0.11	−0.38	−0.27	−1.67
ZnO	Hexagonal a = 3.260 c = 5.080	30	39.5	1.47×10^{-7}	3.20	0.05	−0.77	−2.38	−0.82

SS, specific surface area.

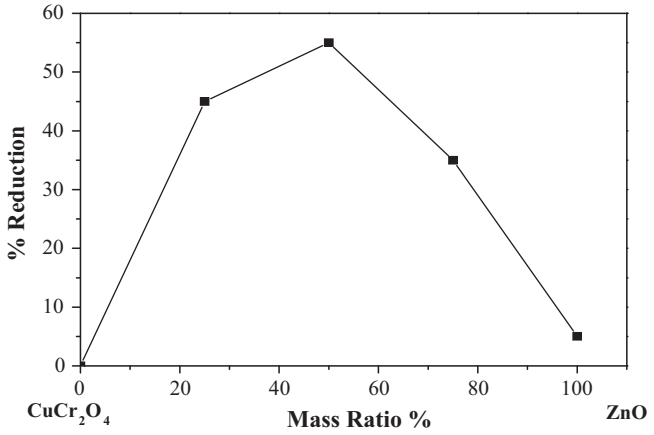

Fig. 6. Influence of the mass ratio ($CuCr_2O_4$/ZnO) on the chromate photo reduction.

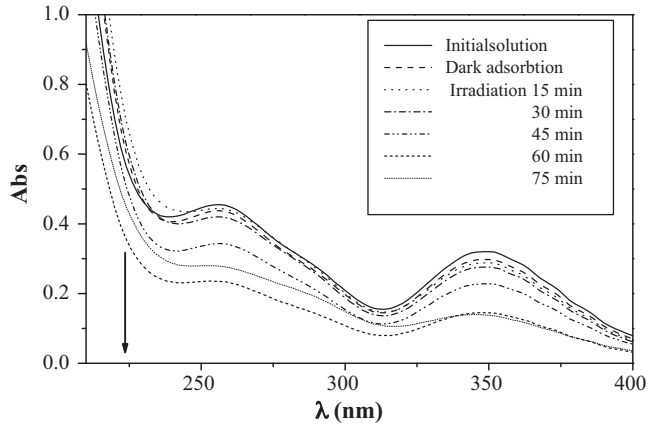

Fig. 7. UV–vis spectra of the chromate solutions over illumination time.

dark. It should be noticed that no photolysis occurs in presence of oxalic acid and the Cr(VI) concentration does not change significantly, it decreases by 2.7% only. The absence of peak at 300 nm in the spectrum of illuminated solution is due to the adsorption of Cr^{3+}. The mineralization occurs via oxidative process by both photo holes and dissolved oxygen which generate reactive OH^* radicals. The pathway generally accepted is the following [16]:

$$O_2(ads) + e^- \rightarrow O_2^{*-} \xrightarrow{H^+} HO_2^* \xrightarrow{HO_2^*} O_2 + H_2O_2 \xrightarrow{e^-} O_2 + OH* + OH^- \quad (7)$$

Oxalic acid is converted through more than one path and hydrogen peroxide is the product of a reaction catalyzed by a large number of oxidases. Such hypothesis is supported by the apparition of an electrochemical peak of O_2/H_2O_2 couple at ~−0.2 V in the J(V) characteristic on ZnO electrode illuminated by UV light under O_2 bubbling (Fig. 8). On the contrary, the photoactivity is found to be negligible and the peak disappears in N_2 saturated solution. The quantum efficiency (η) is given by:

$$\eta = 3\left\{\frac{\text{number of converted } HCrO_4^-(\text{mol s}^{-1})}{\text{photons flux}(s^{-1})}\right\}$$

A η value of 0.15% is found. There is a real desire to develop a large-scale photo electrochemical conversion to harness the solar energy and experiment under direct insolataion (solar constant, AM1) is conducted to compare the results with the artificial light (Fig. 9).

Table 2
Pseudo-first-order kinetics constants, correlation coefficient (R^2) and half life time at different initial concentrations of Cr(VI).

C_o (mol/L) × 10^4	R^2	k_{app}	$t_{1/2}$ (min)
0.679	0.992	0.030	21.096
1	0.992	0.015	42.178
1.359	0.993	0.006	99.377
1.699	0.985	0.004	152.871
2	0.992	0.002	338.095

3.2. Kinetic study

The chromate reduction is investigated in the range of 20–60 ppm and the process at low concentrations follows a pseudo first order kinetic [17]:

$$r = -\frac{dC}{dt} = k_{app}C \quad (8)$$

The integration of Eq. (8) leads to:

$$\ln\frac{C_o}{C} = k_{app}t \quad (9)$$

C_o being the initial concentration. A linear relationship is observed between $\ln(C_o/C)$ and the reaction time t (Fig. 10), from which the apparent rate constant (k_{app}) and the half life time $t_{1/2}$ are determined (Table 2). The decrease of k_{app} with increasing C_o results simply from blocking photo active sites of the catalyst where only

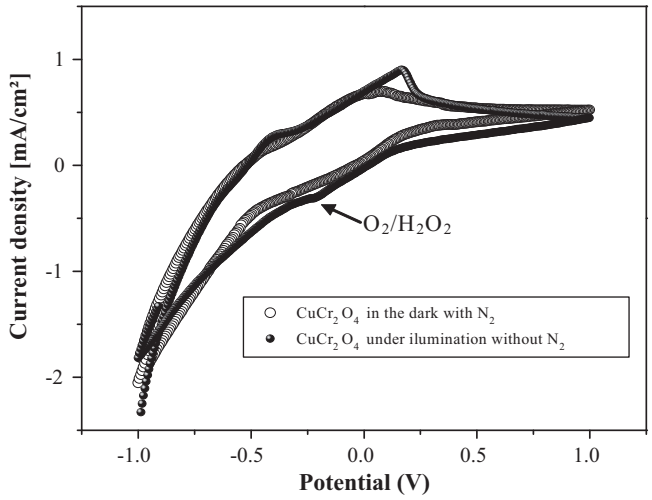

Fig. 8. Cyclic voltammograms of ZnO electrode under light. Scan rate: 0.1 mV s^{-1}.

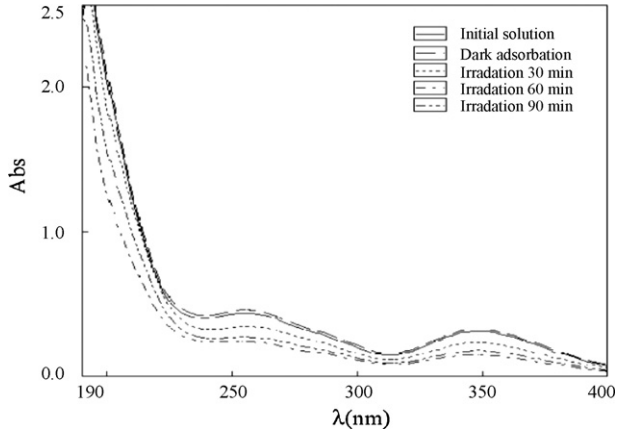

Fig. 9. UV–vis Spectra of the chromate solutions under sun light.

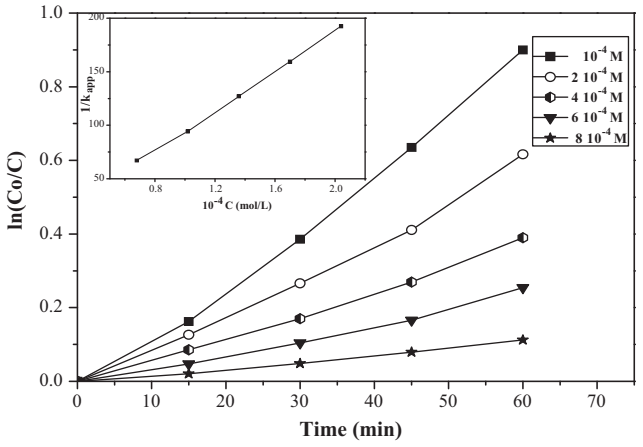

Fig. 10. Kinetics data of photoreduction ($\ln(C_o/C)$ vs. time for different Cr(VI) concentrations (pH ~ 4, 25 ± 1 °C). Inset: the dependence of $1/k_{app}$ on the chromate concentration.

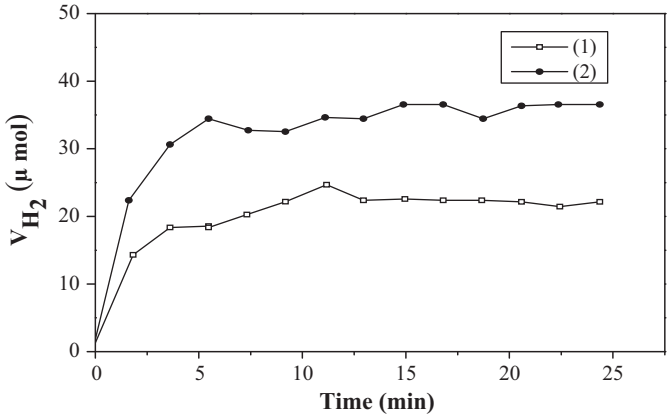

Fig. 11. Volume of evolved H_2 vs. illumination time over the hetero-system: (1) without $HCrO_4^-$, (2) with $HCrO_4^-$.

fewer interact with incident photons. The absorption of light by $HCrO_4^-$ species also accounts in the regression of the photo activity but at a less degree. The photoreduction kinetic is rationalized in terms of the modified Langmuir–Hinshelwood model [18]:

$$\frac{1}{k_{app}} = \frac{1}{k_r k_s} + \frac{C_o}{k_r} \quad (10)$$

the rate constant k_r and the adsorption coefficient k_s are found to be 0.011 mol/min L and 57.187 L/mol (Inset).

The chromate and water reductions occur competitively and this can be understood with the help of the energy diagram (Fig. 4). The environmental friendly hydrogen is recognized as being the ideal fuel in the future. For an efficient hydrogen evolution, a cathodic conduction band and good absorption properties in the visible region are needed, two conditions fulfilled by $CuCr_2O_4$. The volume of evolved hydrogen in presence and in absence of chromate can be used to determine the percentage of photo electrons for the $HCrO_4^-$ reduction (Fig. 11). For a concentration of 30 ppm, the reduction takes place by 60% for chromate reduction against 40% for H_2 evolution. In addition, we have noticed that the volume of liberated hydrogen remains small until ~25 min illumination and this means that at the beginning the photo electrons are in majority consumed by the chromate ions, then the hydrogen starts to evolve.

4. Conclusion

Since the photo activity over oxides is limited and the electron transfer to redox species is quite slow because of the large energy difference between both levels, there is a need to develop other strategies to reach ecological objectives and the hetero-systems seem to be a promising alternative. Hexavalent chromium is highly toxic and the hetero-system $CuCr_2O_4$/ZnO ability for its reduction upon visible illumination has been shown. Our approach is to elaborate the spinel in nano crystalline morphology, via nitrate route. $CuCr_2O_4$ is stable over a fair pH range and works as an electrons reservoir; its major advantage is that a pH change allows an adjustment of the conduction band with respect to ZnO-CB. The reduction is enhanced in presence of oxalic acid, due to efficient separation of (e^-/h^+) pairs and the presence of oxygen is necessary in photocatalysis. The activity dependence on the light intensity is found to be an experimental indicator for the visible light-driven catalysis under direct insulation. The experimental data are well fitted by the modified Langmuir–Hinshelwood model. The Cr(VI) reduction takes place competitively with the water discharge which is partially responsible for the saturation along with the Cr^{3+} oxidation by photolysis.

Acknowledgements

The authors are grateful to Dr. W. Ketir for her help in the characterization of materials and M.B. Bouchali for providing linguistic scrutiny. This work has been financially supported by the Faculty of Chemistry (Algiers).

References

[1] E.A.F.A. Fadigas, J.R. Dias, Desalination 237 (2009) 140–146.
[2] W. Ketir, A. Bouguelia, M. Trari, Water Air Soil Pollut. 199 (2009) 115–122.
[3] D.P. Das, K. Parida, B.R. De, J. Mol. Catal. A: Chem. 245 (2006) 217–224.
[4] E. Gkika, A. Troupis, A. Hiskia, E. Papaconstantinou, Appl. Catal. B: Environ. 62 (2006) 28–34.
[5] P. Mytych, Z. Stasicka, Appl. Catal. B: Environ. 52 (2004) 167–172.
[6] T.T.Y. Tan, D. Beydoun, R. Amal, J. Mol. Catal. A: Chem. 202 (2003) 73–85.
[7] P. Mytych, P. Ciešla, Z. Stasicka, Appl. Catal. B: Environ. 59 (2005) 161–170.
[8] R. Brahimi, Y. Bessekhouad, A. Bouguelia, M. Trari, J. Photochem. Photobiol. A: Chem. 186 (2007) 242–247.
[9] S. Boumaza, A. Boudjemaa, A. Bouguelia, R. Bouarab, M. Trari, Appl. Energy 87 (2010) 2230–2236.
[10] K. Chhor, J.F. Boucquet, C. Colbeau-Justin, Mater. Chem. Phys. 86 (2004) 123–131.
[11] S. Saadi, A. Bouguelia, A. Derbal, M. Trari, J. Photochem. Photobiol. A: Chem. 187 (2007) 97–104.
[12] K. Prabhakaran, D.S. Patil, R. Dayal, N.M. Gokhale, S.C. Sharma, Mater. Res. Bull. 44 (2009) 613–618.
[13] N. Nasrallah, M. Kebir, Z. Koudri, M. Trari, J. Hazard. Mater. 185 (2011) 1398–1404.
[14] R. David, Lide Editor-in-Chief Handbook of Chemistry & Physics, 89th ed., 2008–2009.
[15] P. Atkins, L. Jones, Chemistry, Molecules, Matter and Change, 3th ed., Freeman and Company, New York, 1989.
[16] M.A. Behnajady, N. Modirshahla, R. Hamzavi, J. Hazard. Mater. B133 (2006) 226–232.
[17] B. Pare, S.B. Jonnalagadda, H. Tomar, P. Singh, V.W. Bhagwat, Desalination 232 (2008) 80–90.
[18] Y. Li, S. Sun, M. Ma, Y. Ouyang, W. Yan, J. Chem. Eng. 142 (2008) 147–155.